



Discussion

Discussion of “Centrifuge evaluation of the time-dependent behavior of geotextile-reinforced soil walls” by C.M.L. Costa, J.G. Zornberg, B.S. Bueno, Y.D.J. Costa, *Geotextiles and Geomembranes* 44(2016) 188–200



Huabei Liu*, Chunhai Wang

School of Civil Engineering and Mechanics, Huazhong University of Science and Technology, 1037 Luoyu Road, Wuhan, Hubei 430074, China

ARTICLE INFO

Article history:

Received 11 December 2015

Accepted 1 May 2016

Available online 19 May 2016

1. Introduction

The discussers applaud the authors' effort on investigating the long-term responses of geosynthetic reinforced soil (GRS) structures. Particularly, the reported centrifuge test results on the creep behavior of steep GRS slopes with large strain of geosynthetics are a valuable addition to the literature, with which meaningful information on the creep failure of this type of earth structures may be obtained. However, the mechanism of creep failure presented in the discussed paper may not be comprehensive. The authors indicated that the creep response of the sandy backfill soil was one critical factor that initiated the failure. The discussers believe that another mechanism may be more important in the creep failure, which is the strain softening of the sandy backfill coupling with the load redistribution between the geotextile reinforcements and backfill soil. The discussers will organize their argument as follows: after a discussion of the materials behavior, the possibility of strain softening of the backfill soil in the tests will be analyzed, which is followed by a postulate on the creep failure mechanism.

2. Materials behavior

Two types of geotextile reinforcements were employed in the tests. This discussion is focused on the test results using Geotextile A. According to the results of in-isolation tensile tests, its peak strength was only 0.033 kN/m. The reinforced soil slopes using Geotextile A failed at a centrifugal acceleration of around 20g in the

short term tests, and the corresponding prototype strength was only 0.66 kN/m. This value was far from adequate to maintain the equilibrium of the slope before failure. Using ReSSA Version 3.0 software developed by ADAMA Engineering (2008), the discussers carried out a series of limit equilibrium analyses, assuming sand friction angles from 34° to 44°, and investigating two kinds of reinforcement orientation (horizontal or tangential to the failure surface). The mean reinforcement load to maintain equilibrium of the reinforced soil slope in the prototype scale, viz. a factor of safety around 1.0, was in a range of 2.4 kN/m to 4.2 kN/m. One possibility is the confined strength of the non-woven geotextile was much larger (Boyle et al., 1996), or there is some typo in Fig. 4 of the discussed paper.

From Fig. 18 to Fig. 20 of the discussed paper, the authors presented the time dependent strains in the reinforcement layers and compared them to the creep strains in the in-isolation tests. However, the load in a reinforcement layer changed under sustained loading of the reinforced soil structure (Li and Rowe, 2001; Liu and Won, 2009; Liu et al., 2009; Ariyaratne et al., 2013), and the long-term reinforcement strain, strictly speaking, was not the creep strain. From the material's viewpoint and by definition, creep refers to the increase of deformation under constant stress. The changes of reinforcement load in the tests will be discussed later.

Monterey No. 30 sand was used in the tests at a relative density of 70%. The reported peak angle of internal friction was 36.4°. However, in Zornberg et al. (2004), much larger angle of internal friction, $\phi = 41.4^\circ$, was reported for the same soil at similar relative density from triaxial compression tests ($D_r = 75\%$). The discussers understand that there might be variations in the actual soil samples used in the different tests, but since stress–strain relationships of the backfill soil are not provided in the discussed paper, those in

DOI of original article: <http://dx.doi.org/10.1016/j.geotexmem.2015.09.001>.

* Corresponding author. Tel.: +86 27 8755 7960; fax: +86 27 8754 2231.

E-mail addresses: hbliu@hust.edu.cn (H. Liu), h_217@hust.edu.cn (C. Wang).

Zornberg et al. (2004) were employed to explain the soil behavior. According to the stress–strain relationships in the triaxial compression tests (Zornberg et al., 2004), the residual friction angle of the soil was 34°, and the soil exhibited significant strain-softening after the peak strength. Even if the peak friction angle was 36.4°, strain-softening should have occurred when the soil strain was large considering the density of the backfill soil.

In the centrifuge tests, the soil was in a stress state close to the plane-strain condition, and the friction angle of sand in a plane-strain condition is higher than that in a triaxial condition. According to Lade and Lee (1976), the relationship between plane-strain friction angle ϕ_{ps} and triaxial friction angle ϕ_{tr} may be approximated as $\phi_{ps} = 1.5\phi_{tr} - 17$ ($\phi_{tr} > 34^\circ$). Hence the plane-strain friction angle in the centrifuge tests was between 37.6° and 44°.

3. Strain-softening of the backfill soil

For reinforcement layers inside a steep GRS slope, the reinforcement tension T may be represented by Fig. 1 when the slope is under working stress condition and the reinforcement strain is small. Under this condition, there exists a peak reinforcement load T_{max} in each reinforcement layer, which is located at the potential failure surface between the two ends. Before a slip surface is formed at this location, the reinforcement layer can be assumed to remain horizontal. The slope of reinforcement load at this location is zero, which is also equal to the shear stress τ at the soil–reinforcement interface, as shown in Fig. 1 (Liu and Won, 2014; Liu, 2015). The lateral deformations of the backfill and reinforcement are thus compatible at the potential failure surface. Since the shear stress $\tau = 0$, the vertical soil stress σ_z and the lateral soil stress σ_l at the potential failure surface may also be considered as the major and minor principal stresses, respectively.

If the reinforcement layer may still be assumed to remain horizontal when the soil stress reaches its peak strength, it is possible to analyze the lateral soil strain ϵ_l at this stress level. Since the lateral deformations of soil and reinforcement are compatible at the potential failure surface, the lateral soil strain is also equal to the reinforcement strain. To this end, the stress–strain relationship of granular soil before the peak strength and under plane-strain condition can be represented by a hyperbola (Liu and Won, 2014):

$$\sigma_z - \sigma_l = \frac{\epsilon_z}{\frac{1}{kp_a(\sigma_l/p_a)^n} + \frac{R_f(1 - \sin \phi_{ps})}{2\sigma_l \sin \phi_{ps}} \epsilon_z} \quad (1)$$

Here ϵ_z is the vertical soil strain, σ_l is the lateral soil stress, or the confining soil stress, k is the soil parameter that determines the soil

modulus, p_a is the atmospheric pressure, R_f is the failure ratio, $n < 1$ is the modulus exponent, and ϕ_{ps} is the peak friction angle under plane-strain condition (Duncan et al., 1980). The slope of this stress–strain relationship may then be expressed as (Liu and Won, 2014):

$$C_t = kp_a \left(\frac{\sigma_l}{p_a}\right)^n \left[1 - R_f \frac{(\sigma_z - \sigma_l)(1 - \sin \phi_{ps})}{2\sigma_l \sin \phi_{ps}}\right]^2 \quad (2)$$

Relationship between the lateral and vertical soil strain may be represented by the Rowe's stress–dilatancy relationship under plane-strain condition, which is given as (Rowe, 1962; Wood, 1990):

$$\frac{\sigma_z}{\sigma_l} \left| \frac{d\epsilon_z}{d\epsilon_l} \right| = K \quad (3)$$

Here K is the Rowe's dilatancy constant, which may be expressed as $K = 1 + \sin \phi_r / 1 - \sin \phi_r$, with ϕ_r being the residual friction angle (Wood, 1990).

With these relationships and the compatibility condition, an increase in the vertical soil stress $\Delta\sigma_z$ results in an increase in the reinforcement load ΔT (Liu and Won, 2014):

$$\Delta T = J \Delta\sigma_z / \left(K \left(\frac{\sigma_l}{\sigma_z} \right) C_t + \frac{J}{S_v} \right) \quad (4)$$

Here J is the reinforcement stiffness, and S_v is the vertical reinforcement spacing.

The lateral soil strain at peak soil strength may be obtained using Eqs. (1)–(4), by gradually increasing σ_z and varying the reinforcement stiffness such that the lateral soil stress $\sigma_l = T_{max}/S_v$ is small enough to mobilize the peak soil strength. Note that at peak soil strength $\sin \phi_{ps} = \sigma_z - \sigma_l / \sigma_z + \sigma_l$. For this purpose, a relatively large J may be employed as an initial trial, and the corresponding T_{max} and σ_l are calculated with the given overburden soil stress using the procedure in Liu and Won (2014). The mobilized friction angle, $\phi_{mob} = \sin^{-1}[(\sigma_z/\sigma_l - 1)/(\sigma_z/\sigma_l + 1)]$, is then compared with the peak value. If it is smaller, the trial reinforcement stiffness is reduced, and the aforementioned steps are repeated until the peak soil strength is attained.

Using the above procedure and assuming a centrifugal acceleration $N = 19g$, the lateral soil strains for the GRS slope at peak soil strength are shown in Fig. 2. For this analysis, the hyperbolic and stress–dilatancy parameters were based on the triaxial test results of dense Monterey No. 30 sand reported in Zornberg et al. (2004), which are shown in Table 1. It can be seen that the lateral soil strains were smaller than 15%, and it is smaller with lower vertical soil stress. The values in Fig. 2 are illustrative only. Since the same geotextile was used for different reinforcement layers, the peak soil

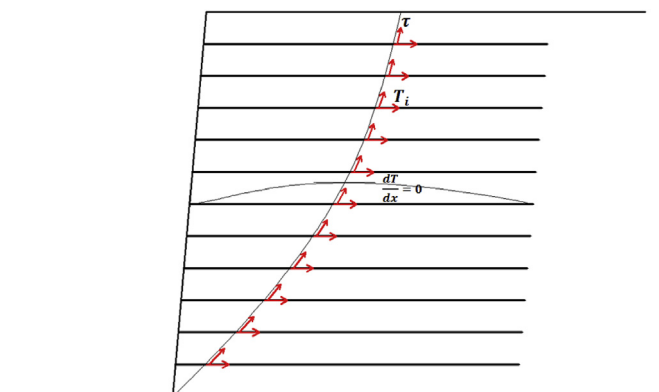


Fig. 1. Illustration of the equilibrium of the GRS slope and the reinforcement load.

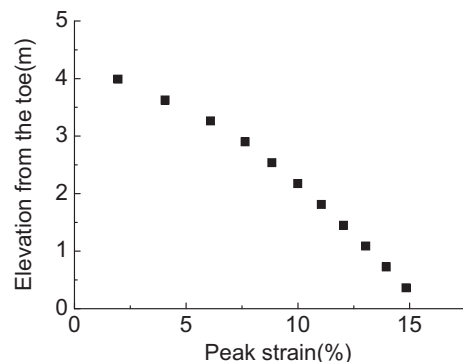


Fig. 2. Lateral soil strains in the GRS slope at $N = 19g$ and at peak soil strength.

strength was mobilized at different g -levels for different elevations. Since the slope failed at $N = 19g$ (Test F2), the g -levels that mobilized the peak soil strength would have been smaller than $19g$, and the corresponding vertical soil stresses would have been smaller than those at $N = 19g$. It is therefore easy to infer that the lateral soil strains were smaller than 15% at peak soil strength in the centrifuge tests, provided that the soil parameters were accurate in the analysis. Since the lateral deformations of soil and reinforcement are compatible at this stress level, the reinforcement strains were also smaller than 15% at peak soil strength in the tests.

Considering the uncertainty in the soil parameters, it is expected that the actual reinforcement strains at peak soil strength in the tests were not the same as those analyzed in this discussion. But it is clear that they were smaller than 40%, around which the slopes failed in the centrifuge tests. In another word, the soil at the failure surface experienced considerable straining beyond the peak soil strength, and strain-softening should have occurred considering the dense state of the backfill soil.

When the reinforcement strain was as large as 40%, it is expected that the soil at the failure surface was at the residual state. That is, considerable sliding must have occurred along the failure surface. With $\phi_r = 34^\circ$ (Zornberg et al., 2004), the stability of the GRS slope at $N = 19g$ was analyzed by the ReSSA software (ADAMA Engineering, 2008). Since the slope had slid significantly, the reinforcement layers were assumed to be tangent to the failure surface. The resulted failure surface at a factor of safety = 1.01 is given in Fig. 3, together with the measured rupture surface in Test F2. The two surfaces are very close to each other. The mean reinforcement load at this state was found to be 4.17 kN/m.

Fig. 10 of the discussed paper shows that the location at the peak reinforcement strain in a reinforcement layer did not change with an increase in the g -level. Although not reported, it appears that the failure surface was developed under certain g -level, and it did not change location with an increase in the gravity force. The soil slid along the same failure surface after its formation. And the friction resistance along the failure surface should have decreased after the

peak strength had been mobilized, considering the dense state of the backfill soil. This kind of phenomenon is consistent with the finding in Liu and Ling (2012).

4. Long-term behavior of GRS slopes

The long-term tests at low g -levels resulted in stable responses of the GRS slopes, although there was creep displacement. The long-term tests were continued for only 10 h, which is very short compared to the service life of a reinforced soil structure. Extensive experimental and numerical test results have shown that, under working stress condition when the reinforcement strain was small, GRS slopes or walls with granular backfill soils exhibited stable behavior after years of services (Wu and Helwany, 1996; Allen and Bathurst, 2002; Onodera et al., 2004; Liu and Ling, 2007; Liu and Won, 2009; Yang et al., 2009, 2010, 2014; Liu et al., 2009; Liu, 2012; Portelinha et al., 2014). Creep displacement developed after the end of construction, but it ceased to increase after a few years. Liu and Won (2009) and Liu et al. (2009) have discussed this issue, and it was pointed out that creep behavior of GRS structures was the result of long-term interaction between soil and geosynthetic reinforcement. The creep rate of granular soil was much smaller than that of geosynthetics (Becker and Nunes, 2015), and the loading was transferred from the reinforcement layers to the backfill soil. Most of the reinforcement layers experienced load relaxation instead of creep deformation when the GRS structure was subjected to constant loading.

However, the above analysis only applies when the reinforcement strain is small such that the soil deformation has not mobilized the peak soil strength. If short-term loading leads to strain softening of the backfill soil at the failure surface, sustained loading afterwards may initiate failure when the creep rate of geosynthetics is higher than that of the backfill soil. As pointed out by the authors in Fig. 22 of the discussed paper, the creep rate of geosynthetics is at least 10 times higher than that of sand. Therefore, the following postulate may be established to explain the creep failure in Tests C4 and C8.

At a g -level equal to $80\%N_f$, N_f being the one at short-term failure, the reinforcement strains were larger than the ones to mobilize the peak soil strength, as shown in Fig. 14 of the discussed paper. The soil was therefore mostly at the state of strain-softening. Since the geotextile exhibited considerable time-dependent property, the reinforcement strain further developed with constant loading, and the soil further slid along the failure surface, resulting in larger soil strain. The shear resistance τ at the failure surface then decreased due to strain softening (Fig. 1), which in turn increased the load T_i in the reinforcement, so that the sliding soil mass might be in equilibrium. Reinforcement strain further developed with a larger T_i , soil sliding further increased, and the shear resistance τ further decreased. This trend continued, until the residual soil strength was reached, and the long-term reinforcement strength was not adequate to maintain equilibrium of the soil mass. During this process, the orientation of T_i changed from horizontal to tangential to the failure surface.

The discussers carried out another limit equilibrium analysis using ReSSA 3.0 (ADAMA Engineering, 2008). The g -level employed was 16g, which was approximately the one in Test C4. The soil friction angle was 34° . At a factor of safety around 1.0, the failure surface is illustrated in Fig. 3, which was close to the one at short-term failure. The mean reinforcement load was 2.91 kN/m. This result showed that at creep failure of the GRS slope, the soil was at its residual state.

The aforementioned postulate does not consider the time-dependent behavior of the backfill soil. It is possible that the creep rate of the backfill soil was higher after the peak soil strength

Table 1
Soil parameters.

Unit weight (kN/m ³)	ϕ_{ps}	K	k	n	R_f
16.1	44	3.54	1300	0.455	0.867

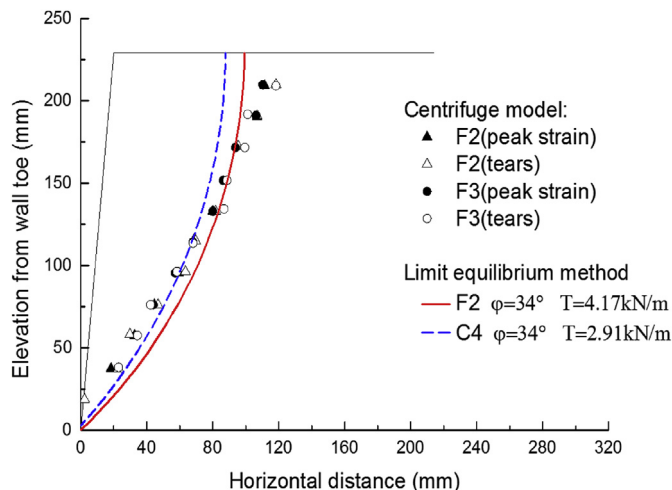


Fig. 3. Comparison of failure surfaces in the centrifuge tests and from limit equilibrium analyses (the dimension is in the model scale).

had been mobilized. However, for granular soils, it is not expected that the creep rate would be higher than or close to that of the geotextile. Therefore, the load redistribution between soil and geotextile as discussed above should have been valid even with time-dependent behavior of the backfill soil.

5. Conclusions

A postulate of creep failure of GRS slopes with large reinforcement strain was proposed in this discussion. The discussers believe that the strain-softening of dense backfill soil have contributed to the creep failure, together with the time-dependent interaction between soil and geotextile reinforcement. This postulate implies that the stress level in the backfill soil should be smaller than its peak strength under working stress condition. Therefore, conservatism in the current design practice may be needed. This conclusion is similar to the one in the discussed paper, but is based on different mechanisms.

Acknowledgment

The study was supported by the National Natural Science Foundation of China (Grant No. 51379082). The support is gratefully acknowledged. The discussers also would like to thank Dr. Dov Leshchinsky for providing the ReSSA 3.0 software for the analyses.

References

- ADAMA Engineering, Inc, 2008. ReSSA Software Version 3.0. Newark, Delaware, USA.
- Allen, T.M., Bathurst, R.J., 2002. Observed long-term performance of geosynthetic walls, and implications for design. *Geosynth. Int.* 9 (5–6), 567–606.
- Ariyaratne, P., Liyanapathirana, D.S., Leo, C.J., 2013. Effect of geosynthetic creep on reinforced pile-supported embankment systems. *Geosynth. Int.* 20 (6), 421–435.
- Becker, L.B., Nunes, A.L.L.S., 2015. Influence of soil confinement on the creep behavior of geotextiles. *Geotext. Geomembr.* 43 (4), 351–358.
- Boyle, S.R., Gallagher, M., Holtz, R.D., 1996. Influence of strain rate, specimen length and confinement on measured geotextile properties. *Geosynth. Int.* 3 (2), 205–225.
- Duncan, J.M., Byrne, P., Wong, K.S., Mabry, P., 1980. Strength, Stress Strain and Bulk Modulus Parameters for Finite Element Analyses of Stresses and Movements in Soil Masses. Geotechnical Engineering Research Rep. No. UCB/GT/80-01. Univ. of California—Berkeley, Berkeley, CA.
- Lade, P.V., Lee, K.L., 1976. Engineering Properties of Soils. Rep. No. UCLA-ENG-7652. Univ. of California—Los Angeles, Los Angeles.
- Li, A.L., Rowe, R.K., 2001. Influence of creep and stress-relaxation of geosynthetic reinforcement on embankment behaviour. *Geosynth. Int.* 8 (3), 233–270.
- Liu, H., 2012. Long-term lateral displacement of geosynthetic-reinforced soil segmental retaining walls. *Geotext. Geomembr.* 32, 18–27.
- Liu, H., 2015. Reinforcement load and compression of reinforced soil mass under surcharge loading. *J. Geotech. Geoenviron. Eng. ASCE* 141 (6), 04015017.
- Liu, H., Ling, H.I., 2007. A unified elastoplastic–viscoplastic bounding surface model of geosynthetics and its applications to GRS-RW analysis. *J. Eng. Mech.* 133 (7), 801–815.
- Liu, H., Ling, H.I., 2012. Seismic responses of reinforced soil retaining walls and the strain softening of backfill soils. *Int. J. Geomech.* 12 (4), 351–356.
- Liu, H., Wang, X., Song, E., 2009. Long-term behavior of GRS retaining walls with marginal backfill soils. *Geotext. Geomembr.* 27 (4), 295–307.
- Liu, H., Won, M.S., 2009. Long-term reinforcement load of geosynthetic-reinforced soil retaining walls. *J. Geotech. Geoenviron. Eng. ASCE* 135 (7), 875–889.
- Liu, H., Won, M.S., 2014. Stress dilatancy and reinforcement load of vertical-reinforced soil composite: analytical method. *J. Eng. Mech. ASCE* 140 (3), 630–639.
- Onodera, S., Fukuda, N., Nakane, A., 2004. Long-term behavior of geogrid reinforced soil walls. In: *Proceedings 3rd Geosynthetics Asia*, Seoul, Korea, pp. 255–264.
- Portelinha, F.H., Zornberg, J.G., Pimentel, V., 2014. Field performance of retaining walls reinforced with woven and nonwoven geotextiles. *Geosynth. Int.* 21 (4), 270–284.
- Rowe, P.W., 1962. The stress–dilatancy relation for static equilibrium of an assembly of particles in contact. *Proc. R. Soc. Lond. Ser. A* 269 (1339), 500–527.
- Wood, D., 1990. *Soil Behaviour and Critical State Soil Mechanics*. Cambridge University Press, Cambridge, U.K.
- Wu, J.H.T., Helwany, S.M.B., 1996. A performance test for assessment of long-term creep behavior of soil–geosynthetic composites. *Geosynth. Int.* 3 (1), 107–124.
- Yang, G., Ding, J., Zhou, Q., Zhang, B., 2010. Field Behavior of a geogrid reinforced soil retaining wall with a wrap-around facing. *Geotech. Test. J.* 33 (1), 96–101.
- Yang, G., Liu, H., Zhou, Y., Xiong, B., 2014. Post-construction performance of a two-tiered geogrid reinforced soil wall backfilled with soil–rock mixture. *Geotext. Geomembr.* 42 (2), 91–97.
- Yang, G., Zhang, B., Lv, P., Zhou, Q., 2009. Behaviour of geogrid reinforced soil retaining wall with concrete-rigid facing. *Geotext. Geomembr.* 27 (5), 350–356.
- Zornberg, J.G., Cabral, A.R., Viratjandr, C., 2004. Behaviour of tire shred – sand mixtures. *Can. Geotech. J.* 41, 227–241.



Reply

Reply from authors Costa, C. M. L., Zornberg, J. G., Y. D. J. Costa.
 “Centrifuge evaluation of the time-dependent behavior of
 geotextile-reinforced soil walls”. *Geotextiles and Geomembranes* 44
 (2016) 188–200



Carina Maia Lins Costa ^{a,*}, Jorge Gabriel Zornberg ^{b,1}, Yuri Daniel Jatobá Costa ^{a,2}

^a Federal University of Rio Grande do Norte, Campus Universitário Lagoa Nova, Natal, RN, 59078-970, Brazil

^b The University of Texas at Austin, Department of Civil Architectural and Environmental Engineering, 301 E. Dean Keeton, Austin, TX, 78712-0280, USA

ARTICLE INFO

Article history:

Received 30 April 2016

Accepted 1 May 2016

Available online 4 June 2016

1. Introduction

The authors thank for the discussers for their comments and appreciate their effort to conduct a series of limit equilibrium analyses to prepare a discussion of the results of the paper. The authors are pleased for the opportunity to provide some additional discussion about the time-dependent mechanisms that may develop in geosynthetic-reinforced soil structures.

The authors agree with the discussers that strain softening may have contributed to the failure of the centrifuge models. However, the authors believe that the significant consistency between the time-dependent response of the models and the creep response of the geotextiles point to creep as the most probable cause of failure.

The discussers state that: “The authors indicated that creep response of the sandy backfill soil was one critical factor that initiated failure”. However, please note that the authors have not stated such conclusions. Instead, the authors have concluded in the paper that the sand backfill used in the centrifuge models, which is frequently considered as having negligible creep, was found not to prevent the development of time-dependent deformations and, ultimately, failure. That is, the sand backfill was not able to prevent

the observed failure, but the sand backfill itself was not identified as the critical factor to cause or initiate failure.

Additional considerations are provided below regarding time-dependent response of the geosynthetic reinforced models.

2. Time-dependent strains in the geosynthetic-reinforced sand

The rate of the time-dependent strains that developed in the geotextiles before failure of the centrifuge models was found to be remarkably similar to rate of the time-dependent strains in the geotextiles when evaluated using conventional creep tests. The authors emphasize, however, that this behavior should not be generalized to reinforced systems involving other geosynthetics, backfill soils, and structures configurations without significant additional evaluation. In particular, other responses could be obtained depending on a number of factors such as the creep tendency of the reinforcement in relation to that of the soil as well as on the soil shear strength that has been mobilized after loading application. This includes the relevant aspect of post-peak behavior of the backfill soil. The time-dependent behavior of reinforced sand can be evaluated considering the case of a reinforced soil element (unit cell) involving a single reinforcement layer confined between two layers of sand. Assuming strain compatibility between soil and reinforcement, if the element is subjected to a given vertical normal stress, the soil and reinforcement will interact and deform while still ensuring equilibrium.

The sand in the element is considered to exhibit post-peak shear strength loss, which is typical of dense sands. Of particular interest to this discussion is the condition where the tendency of the soil to creep is smaller than that of the reinforcement. Two situations can be expected to develop in this hypothetical geosynthetic-reinforced sand system, depending on soil shear strength that has been initially mobilized. If the soil shear strain that has been mobilized after application of the normal stress is smaller than the strains at peak shear strength, the tendency of the reinforcement to creep will lead to time-dependent strains that would, in turn, lead to an

DOI of original article: <http://dx.doi.org/10.1016/j.geotexmem.2016.05.002>.

* Corresponding author. Tel.: +55 84 33422496; fax: +55 84 3215 3703.

E-mail addresses: cmlins@gmail.com, carina@ct.ufrn.br (C.M.L. Costa), zornberg@mail.utexas.edu (J.G. Zornberg), ydjcosta@ct.ufrn.br (Y.D.J. Costa).

¹ Tel.: +1 512 232 3595; fax: +1 512 417 6548.

² Tel.: +55 84 33422496; fax: +55 84 3215 3703.

increase in soil shear stresses. As higher soil shear stresses are mobilized, the reinforcement tension will decrease. That is, time-dependent strains correspond, in this case, to time-dependent decreases in the reinforcement tension. This type of response is likely to occur in geosynthetic-reinforced soil walls under working stress conditions. It should be noted that the reinforcement tension will decrease to the point in which the soil reaches its peak shear strength.

On the other hand, if soil shear strain exceeds its peak shear strength, subsequent time-dependent strains (because of the reinforcement tendency to creep) would lead to the loss of soil stress. That is, time-dependent strains correspond, in this case, to time-dependent increases in the reinforcement tension which are needed to ensure equilibrium. This mechanism may ultimately lead to failure of the reinforced soil element.

It should be noted that the previous discussion considered an “element” of reinforced sand. However, the soil strength depends on several factors, including the stress path. Indeed, the behavior of geosynthetic-reinforced walls is more complex due to the interaction among multiple reinforcement layers and the effect of other wall components. For instance, time-dependent stress redistribution may occur among layers. The tension in a specific reinforcement layer may be redistributed to other layers that may have been subjected to smaller tension. Consequently, as stress redistribution occurs, the layer initially subjected to higher stresses would exhibit stress relaxation (decrease in stress with time under constant strains) or, most probable, time-dependent strain with load decreasing.

3. Failure of the geosynthetic-reinforced sand models

The discussers posed some questions regarding the strength properties of the geotextiles and sand used in the centrifuge models. It should be noted that there is no typo in Fig. 4, which provides the values obtained from tensile tests conducted without confinement (ASTM D4595, 2011). The effect of confinement on tensile properties of geotextiles has been recognized by the authors, and corresponds to a confined geotextile strength of 0.124 kN/m (2.48 kN/m in the prototype scale). This magnitude of confined strength is consistent with the range of values considered by the discussers in their analyses using the ReSSA software. The adopted confined strength value is based on the evaluations conducted by Arriaga (2003), who conducted centrifuge tests on reinforced slopes using the same geotextile and backfill sand used by the authors. The value of peak friction angle from triaxial tests is 36.4°, as reported by the authors in the paper. Although the tests did not reach strain values that are large enough to guarantee a critical state condition, the friction angles at large strains appear to have converged to a residual value of approximately 32.5°. These values are consistent with those reported by Zornberg et al. (1998) for the Monterey No. 30 sand.

The stability analyses conducted by the discussers were performed using the shear strength results obtained from triaxial test on backfill sand. However, the authors believe that the significance of soil strain softening in the observed performance of the centrifuge models may not be as relevant as that considered by the discussers. Insight can be gained from comparison of shear strength results obtained from triaxial tests conducted using reinforced and pure soil specimens. The comparisons have often been reported to show a different post-peak response in the case of tests conducted using reinforced and unreinforced soil specimens. For example, laboratory triaxial compression tests carried out by Latha and Murthy (2007) and by Haeri et al. (2000) have shown a

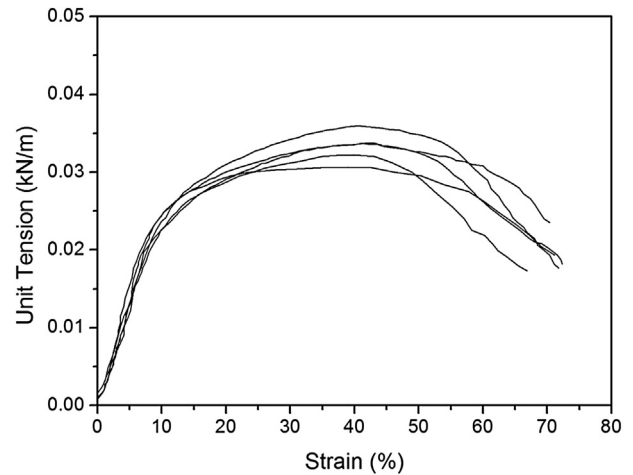


Figure 4. Results of tensile tests conducted in the cross-machine direction using Geotextile A.

significantly smaller post-peak shear strength loss when using reinforced sand than when testing unreinforced sand specimens. Specifically, the presence of reinforcement inclusions was reported in these studies to affect deformation mechanism and the development of shear bands. Haeri et al. (2000) show images of failed triaxial specimens that illustrate different failure patterns for reinforced and unreinforced sands. In particular, the reinforced sand specimens showed larger axial strains at failure. However, the observation of the images of failed specimens suggests smaller soil shear strains in reinforced sand when compared to soil shear strain in unreinforced sand. Thus, it is likely that the comparatively smaller soil shear strains in reinforced sand are associated to smaller post-peak shear strength loss than in unreinforced sand. Accordingly, despite the comparatively high strain levels reached in the models, the impact of strain softening may not be very significant, based on typical post-peak shear strength behavior of reinforced triaxial specimens.

Experimental results from reduced-scale models of reinforced soil slopes tested in a geotechnical centrifuge obtained by Zornberg et al. (1998) also suggest that the soil strain softening that develops in reinforced sand differs from that observed in unreinforced soil. The researchers concluded that the mobilized friction angle at the time of failure in the centrifuge reinforced soil models corresponded to the peak shear strength. This issue was extensively discussed by Zornberg (2002), who evaluated the results from reinforced soil slopes centrifuge models constructed using Monterey No. 30 sand. The models evaluated in that study were identical, other than having been built using two different relative densities for backfill soil. The backfill material of a sand placed under two relative densities has different peak shear strength, but the same residual shear strength. Since models with higher relative density (that is, higher peak friction angle) failed at a higher g -level, the peak friction angle was identified as the shear strength parameter that governed the collapse of the geosynthetic reinforced models. The same conclusion was reached by and Arriaga (2003), also considering the results of centrifuge models involving reinforced soil slopes built using Monterey No. 30 sand. It should be noted that the strain levels in the reinforcements reported by Arriaga (2003) were comparatively high ($\epsilon = 40\%$). As pointed out by Zornberg (2002), “a plausible explanation of these experimental results is that, although the soil may have reached active state due to large horizontal strains because of the extensible

nature of the reinforcements, large shear strains (and drop from peak to residual soil shear strength) only take place along the failure surface during final sliding of the active reinforced wedge”.

Ultimately, the soil post-peak shear strength loss in the models evaluated in the study presented by the authors is expected to have been less significant than that observed in typical triaxial tests of unreinforced soil specimens.

4. Conclusions

The authors concur with the discussers about the potentially detrimental effect of post-peak shear strength losses in the soil backfill. However, while strain softening may have contributed to the failure of the models, the significant consistency between the time-dependent response of the models and the creep response of the geotextiles point to creep as the most probable cause of failure. Indeed, the authors consider that strain softening is a relevant phenomenon among several time-dependent interaction

phenomena between soil and geotextile reinforcement. Overall, the authors believe that both the paper and the discussion lead to similar practical implications in reinforced soil design. Namely, that the level of conservatism that has been adopted in current design practice may be the appropriate one for reinforced soil structures.

References

- Arriaga, F., 2003. Response of Geosynthetic-reinforced Structures Under Working Stress and Failure Conditions. Ph.D. Thesis. University of Colorado at Boulder, Boulder, Colorado, USA, 205 pages.
- Haeri, S.M., Noorzad, R., Oskoorouchi, A.M., 2000. Effect of geotextile reinforcement on the mechanical behavior of sand. *Geotext. Geomembranes* 18 (6), 385–402.
- Latha, G.M., Murthy, V.S., 2007. Effects of reinforcement form on the behavior of geosynthetic reinforced sand. *Geotext. Geomembranes* 25 (1), 23–32.
- Zornberg, J.G., 2002. Peak versus residual shear strength in geosynthetic-reinforced soil design. *Geosynth. Int.* 9 (4), 301–318.
- Zornberg, J.G., Sitar, N., Mitchell, J.K., 1998. Limit equilibrium as basis for design of geosynthetic-reinforced slopes. *J. Geotechnical Geoenvironmental Eng.* 124 (8), 684–698.